Structural and electrical characterization of annealed $Si_{1-x}C_x$/SiC thin film prepared by magnetron sputtering*

Huang Shi-Hua(黄仕华)† and Liu Jian(刘 剑)

Physics Department, Zhejiang Normal University, Zhejiang 321004, *China*

(Received 8 August 2013; revised manuscript received 31 October 2013; published online 1 April 2014)

Si-rich $Si_{1-x}C_x$/SiC multilayer thin films are prepared using magnetron sputtering, subsequently followed by thermal annealing in the range of 800–1200 °C. The influences of annealing temperature (T_a) on the formation of Si and/or SiC nanocrystals (NCs) and on the electrical characteristics of the multilayer film are investigated by using a variety of analytical techniques, including X-ray diffraction (XRD), Raman spectroscopy and Fourier transform infrared spectrometry (FT-IR), current–voltage (I–V) technique, and capacitance-voltage (C–V) technique. XRD and Raman analyses indicate that Si NCs begin to form in samples for $T_a \geq 800$ °C. At annealing temperatures of 1000 °C or higher, the formation of Si NCs is accompanied by the formation of SiC NCs. With the increase in the annealing temperature, the shift of FT-IR Si–C bond absorption spectra toward a higher wave number along with the change of band shape can be explained by a Si–C transitional phase between the loss of substitutional carbon and the formation of SiC precipitates and a precursor for the growth of SiC crystalline. The C–V and I–V results indicate that the interface quality of $Si_{1-x}C_x$/SiC multilayer film is improved significantly and the leakage current is reduced rapidly for $T_a \geq 1000$ °C, which can be ascribed to the formation of Si and SiC NCs.

Keywords: SiC, magnetron sputtering, annealing, leakage current

PACS: 81.15.Cd, 78.55.Ap, 68.55.A–, 81.40.Ef **DOI:** 10.1088/1674-1056/23/5/058105

1. Introduction

Materials consisting of silicon nanocrystals (Si NCs) embedded in a dielectric matrix have attracted considerable interest in the field of silicon optoelectronics.[1–5] Current research on Si NCs is focused on the preparation of Si NCs embedded in oxide, nitride, and carbide hosts.[6–10] Compared with Si NCs embedded in oxide and nitride matrices, the barrier height between Si NCs and amorphous SiC matrix is lower, which can enhance the tunneling probability of carriers between adjacent NCs and effective carrier mobility.[11] Therefore, SiC is an attractive alternative Si-NC host material for solar cell applications due to its low band gap relative to SiO_2 and Si_3N_4.[12] Due to the presence of high trap/state density in SiC matrix, the electrical characteristics of a Si-NC solar cell are seriously poorer than that predicted in Ref. [12]. Understanding trap state generation and oxide charge trapping mechanisms is fundamental to achieving a robust scheme for SiC-based photoelectric devices. To the best of our knowledge, a few reports that combine the structural properties with the electrical characteristics have been published. In order to further improve device performance, it is crucial to understand the electronic properties of Si NCs embedded in amorphous SiC matrix together with their microstructures and optical properties.

Si NCs embedded in a SiC matrix can be formed using high-temperature annealing of a single Si-rich SiC precursor layer.[3,13] Compared with a single precursor layer, Si-rich $Si_{1-x}C_x$/SiC multilayer is expected to offer a better regulation of Si-NC size, owing to the constraint by the thickness of the Si-rich layer. This case is similar to Si-NC formation in SiO_2 or Si_3N_4 matrix reported elsewhere.[14,15] In this work, Si NCs embedded in a SiC matrix are prepared by alternating deposition of Si-rich and near-stoichiometric silicon carbide $Si_{1-x}C_x$/SiC multilayers on Si substrates using magnetron sputtering deposition, followed by post-annealing at 800–1200 °C. In order to investigate electrical properties of $Si_{1-x}C_x$/SiC thin films, current–voltage (I–V) and capacitance–voltage (C–V) measurements are carried out. The structural characteristics of these films are characterized using X-ray diffraction (XRD), Raman spectroscopy, and Fourier transform infrared spectrometry (FT-IR). Based on the relation between electrical and structural characteristics, we have discussed the interface quality and leakage current characteristics of $Si_{1-x}C_x$/SiC multilayer film. In addition, the influence of a thermal annealing process of these thin films on their properties is investigated.

2. Experimental procedure

Si-rich $Si_{1-x}C_x$/SiC thin films were prepared using magnetron sputtering on p-type polished Si wafers (100) with re-

*Project supported by the National Natural Science Foundation of China (Grant No. 61076055), the Open Project Program of Surface Physics Laboratory (National Key Laboratory) of Fudan University, China (Grant No. FDS-KL2011-04), the Key Science and Technology Innovation Team of Zhejiang Province, China (Grant No. 2011R50012), and the Key Laboratory of Zhejiang Province, China (Grant No. 2013E10022).

†Corresponding author. E-mail: huangshihua@zjnu.cn

© 2014 Chinese Physical Society and IOP Publishing Ltd

sistivity of 3–5 Ω·cm. According to the diameter of the SiC target, the pure Si wafer was cut into a sector piece (5% in volume), and then tightly pressed onto the SiC target. The SiC target with a sector piece of Si wafer is used as the Si/SiC target with a diameter of 60 mm. One cathode, which was connected to a SiC target, was powered by a 13.56-MHz radio frequency voltage and the other, which was connected to a Si/SiC target, was powered by a direct current voltage. The sputtering chamber and the pretreatment chamber were first evacuated down to 1.0×10^{-4} Pa before the introduction of the argon gas. In order to eliminate the oxide and water vapor absorbed on the surface of the targets, they were sputtered in the sputtering chamber for 10 min before the growth of $Si_{1-x}C_x$/SiC multilayer films. The typical $Si_{1-x}C_x$/SiC multilayer structure consisted of 20 pairs of alternately stacked 5-nm-thickness $Si_{1-x}C_x$/SiC layers and 5-nm-thickness SiC layers. The thickness of $Si_{1-x}C_x$/SiC layer or SiC layer was controlled by adjusting sputtering power and sputtering time. After deposition, the as-deposited samples were annealed at temperature ranging from 800 to 1200 °C for about 30 min in argon ambient. MIS structures were designed in order to study the electrical characteristics of the annealed and unannealed films. In these structures, electrical contacts were created by evaporating Al on the back side of the silicon wafer and through circular Al dots, 0.5 mm in diameter, deposited with a mechanical mask on the $Si_{1-x}C_x$/SiC films.

The deposition thickness of $Si_{1-x}C_x$ or SiC single layer was estimated by using an Alpha-step profile meter (KLA-Tencor P-10). *C–V* measurements were carried out at a frequency of 1 MHz using a precision LCR meter (Agilent, 4284A) and small sinusoidal test signal of 50 mV. *I–V* measurements were performed by using a sourcemeter (Keithley, 2601). The film structure was investigated by XRD performed on a Philips X'Pert PW 3040/60 diffractometer using Cu Kα radiation ($\lambda = 0.154056$ nm). Raman scattering spectra of the films were found by using a micro-Raman setup (Renishaw, 2000) in backscattering configuration. FT-IR absorption spectra were measured by using a spectrometer (Nicolet, Nexus670). All the measurements were carried out at room temperature (RT).

3. Results and discussion

Figure 1 shows the XRD spectra of the $Si_{1-x}C_x$/SiC films deposited at RT and subsequently annealed at 800–1200 °C, respectively. For the samples deposited at room temperature, only a very broad and weak XRD peak located at 28.40 is observed, which indicates that the crystal structure of the as-deposited film is amorphous. In the case of the annealing temperature of 800 °C, the peak intensity at 28.40 increases rapidly, and its full width at half maximum (FWHM) is 2.30, which indicates that Si NCs begin to form when the annealing temperature increases to 800 °C. When T_a is larger than 1000 °C, two XRD peaks located at 28.40 and 35.60 are observed, and they are attributed to Si (111) plane and SiC (111) plane, respectively.[16,17] With the increase of T_a from 1000 °C to 1200 °C, the FWHM of the XRD peak at 28.40 decreases from 1.10 to 0.40, and its intensity enhances greatly. The XRD peak located at 35.60 begins to emerge when annealing temperature increases to 1000 °C. However, it can be clearly observed at the annealing temperature of 1200 °C, which indicates that SiC NCs have formed. In addition, another XRD peak located at 47.300 was also observed, and assigned to the Si (220) plane. As the size broadening effect is the dominant contributor to XRD profile broadening, the diffraction domain size (D) is estimated by means of the well-known Scherrer's formula: $D = K\lambda/\beta\cos\theta$, where K is a constant to account for the geometry of crystallite (~ 0.89), λ is the X-ray excitation wavelength, and β is the corrected FWHM of the XRD peak after fitting to a Cauchy profile. According to the XRD peak located at 28.40 and 35.60 annealed at 1200 °C, the average grain sizes of Si and SiC NCs are estimated to be about 4.3 and 5.6 nm, respectively. However, the calculated results are usually influenced by inhomogeneous strain and other defects in the structure.

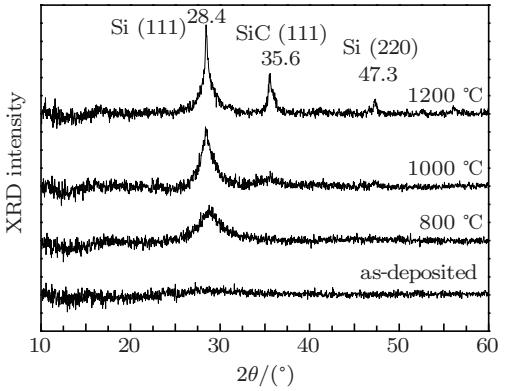


Fig. 1. XRD spectra of $Si_{1-x}C_x$/SiC films deposited at RT and subsequently annealed at 800–1200 °C, respectively.

Raman spectra based on inelastic light scattering is a powerful and non-destructive technique for the analysis of stress, crystal lattice disorder, and homogeneity of materials. It is also an excellent method for studying nanostructured materials due to its high sensitivity to the crystal potential fluctuations and local atomic arrangement. Variations in the disorder and particle size change the shapes and positions of Raman lines. Figure 2 shows the Raman spectra of the $Si_{1-x}C_x$/SiC films deposited at RT and subsequently annealed at 800–1200 °C, respectively. For the film deposited at RT, a broad and weak Raman peak located at 480 cm^{-1} is observed, and this peak is attributed to the transverse optical (TO) mode of amorphous Si. In the case of the annealing temperature of 800 °C, the peak

intensity at 480 cm^{-1} increases rapidly. It is also noteworthy that a very weak peak located at 501 cm^{-1} is seen, which indicates that Si NCs begin to form when the annealing temperature increases to 800 °C. When the annealing temperature is 1000 °C, the peak intensity at 480 cm^{-1} decreases, and that at 506 cm^{-1} increases rapidly. It indicates that the content of amorphous Si decreases and that of nanocrystal Si increases. Meanwhile, a very broad peak located at about 950 cm^{-1} can be observed, and is associated with the longitudinal optical (LO) phonon band of SiC crystalline bands.[18–21] Moreover, this broad peak observed around 950 cm^{-1} may be also associated the second-order Raman band of silicon coexisting at 970 cm^{-1}.[22] However, only a broad Raman peak centered at 940 cm^{-1} was observed in Ref. [21] for a SiC film annealed at temperature higher than 900 °C, and showed features similar to that observed in this work. In Ref. [21], this broad peak was attributed to the longitudinal optical phonon band of microcrystalline SiC. Therefore, the Raman peak located around 950 cm^{-1} can be explained by the changes in the SiC bonding states from amorphous to nanocrystalline with increasing annealing temperature higher than 1000 °C. This is also supported by the above XRD results that show the presence of a SiC nanocrystalline phase in the film annealed at the temperature higher than 1000 °C. When the annealing temperature increases to 1200 °C, the intensity of the Raman peak at 480 cm^{-1} is strong and its FWHM is small. Also, the broad peak at 480 cm^{-1} vanishes. This indicates that the all-crystal structure of Si in the film is nanocrystal Si phase and there is no amorphous Si phase at the annealing temperature of 1200 °C. Meanwhile, the SiC Raman peak becomes sharp and its intensity is enhanced as compared with that annealed at 1000 °C, which is assigned to the formation of SiC NCs.

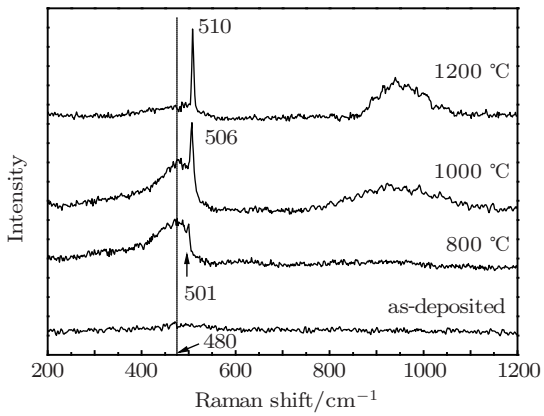


Fig. 2. Raman spectra of SiC thin films deposited at room temperature and subsequently annealed at 800–1200 °C, respectively.

FT-IR spectra were employed to investigate the bonding configuration of as-deposited and annealed $Si_{1-x}C_x$/SiC thin films. For the as-deposited film at RT, a broad absorption peak centered at 710 cm^{-1} can be observed in Fig. 3, and the peak shape can be fitted by a Gaussian line. The Gaussian contribution is ascribed to the disordered silicon–carbon bonds in amorphous SiC.[23,24] For films annealed at temperature higher than 1000 °C, this peak shifts from 710 to 742 cm^{-1}, and the peak shape can be best fitted by a combination line of a Lorentzian and a Gaussian. The shift of peak along with the change of band shape is due to the formation of more Si–C bonds from dangling C and Si bonds.[25] With the increase in the annealing temperature, this peak shifts to 766 cm^{-1} when the sample was annealed at 1200 °C. The peak at 766 cm^{-1} is related to the stretching mode of Si–C bond, which is assigned to the crystalline phase.[26] Upon increasing annealing temperature, the shift of peak position to higher wavenumber indicates that there is a Si–C transitional phase between the loss of substitutional carbon and the formation of SiC precipitates, and a precursor for the growth of SiC crystalline can be assumed.[27] The full width at half maximum (FWHM) of the Si–C peak decreases with increasing annealing temperature, which results from the formation of more Si–C bonds from dangling C and Si bonds.[13] For the film annealed at temperature higher than 1000 °C, the peak intensity evidently increases with the increase in the annealing temperature. This phenomenon can be explained by a change in the film microstructure from an amorphous phase to a nanocrystalline phase, i.e., there is an improved fraction of crystallized SiC in the films when the sample was annealed at 1200 °C. In addition, the absorption peaks are also observed around 456 and 1051 cm^{-1}, which are attributed to the stretching vibrations of Si–O.[28,29] The Si–O absorption band might be due to the film surface oxide formed during high-temperature annealing,[29] which indicates that the annealed film contains oxygen-related defects.

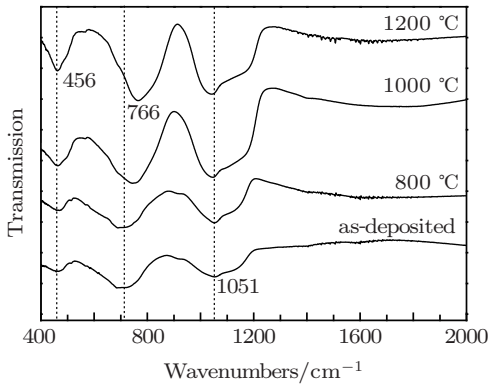


Fig. 3. FT-IR spectra of $Si_{1-x}C_x$/SiC films deposited at RT and subsequently annealed at 800–1200 °C, respectively.

The *C–V* measurement is an important means to characterize the electrical characteristics of the MIS structure. Figure 4 shows *C–V* characteristics of MIS structures fabricated with SiC films obtained at different annealing temperatures. For as-deposited sample, a region of deep depletion can be

obtained from the *C–V* curve, which results from the quick leakage of electrons through the SiC films. The edge is ascribed to the existence of the surface states in the SiC film.[30] The leakage current in the accumulation region decreases with the increase in the annealing temperature. When a very negative gate bias is applied to the p-type Si substrate, holes are attracted to the $Si_{1-x}C_x$/SiC interface. Meanwhile, the accumulated negative charges at the gate side flow through the SiC layer, which decreases the hole density at the $Si_{1-x}C_x$/SiC interface. With the increase in the applied gate bias, the accumulated positive charge vanishes and a negative depletion region begins to form in the silicon. This behavior causes a decrease in the leakage current and an increase in the capacitance, which results in the formation of the peak in the *C–V* curve shown in Fig. 4. The as-deposited sample presents a high leakage current regime, which results in the decrease in the accumulation capacitance. After annealing at 1000 °C, the *C–V* curves do not show the decrease in accumulation capacitance, which results in a rapid reduction of the leakage current.

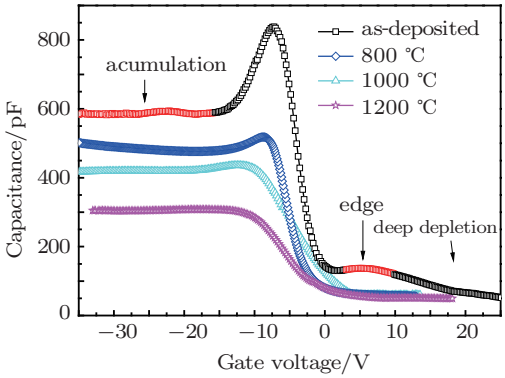


Fig. 4. (color online) *C–V* characteristics of MIS structures fabricated with SiC films obtained at different annealing temperatures.

As shown in Fig. 5, the leakage current of $Si_{1-x}C_x$/SiC thin film significantly decreases after the annealing treatments. When the annealing temperature increases from 800 to 1000 °C, the leakage current descends rapidly. However, the leakage current decreases slowly with the increase in the annealing temperature beyond 1000 °C, which indicates that there is a structural transformation of the films annealed at 1000 °C. From the analysis of XRD, Raman spectra, and FT-IR spectra, the crystallization of SiC starts to form when the annealing temperature is greater than 1000 °C. Therefore, the reduction of the leakage current for the sample annealed at the temperature higher than 1000 °C can be assigned to the formation of Si and SiC NCs.

During the sputtering process, the vitreous network of SiC may be broken down, and the sputtered Si and SiC are the amorphous structure. The break of the bonding arrangement is a precondition of the nanocluster formation. There are local defects in the sputtered $Si_{1-x}C_x$/SiC film and high interface state between $Si_{1-x}C_x$/SiC amorphous film and Si crystalline substrate. These defects are often associated with dangling bonds, surface steps, or defects created by entropy effects in the otherwise smooth interface. The balance between damage and annealing is linked in a particular way to the cluster generation. Thus, interface quality is connected with nanocluster arrangement and configuration. The sputtered Si diffuses during the annealing process and may agglomerate at silicon carbide matrix, which serves as nucleation centers for the growth of the Si NCs. Diffusion during the annealing process leads to a pileup of silicon at the Si-SiC interface. The thermal emission rate from NCs is smaller than that from defects, and then the contribution to the leak current of NCs is lower than that of defects. The amorphous phase of $Si_{1-x}C_x$/SiC film transforms to crystalline phase after annealing at temperature higher than 1000 °C. Meanwhile, the morphological quality of interface between $Si_{1-x}C_x$/SiC multilayer film is improved significantly. On the other hand, traces of oxygen or water vapor in the annealing ambient diffuse into the $Si_{1-x}C_x$/SiC film from the surface. This might result in the oxidation of Si close to the surface of Si substrate, causing a further improvement of interface quality.

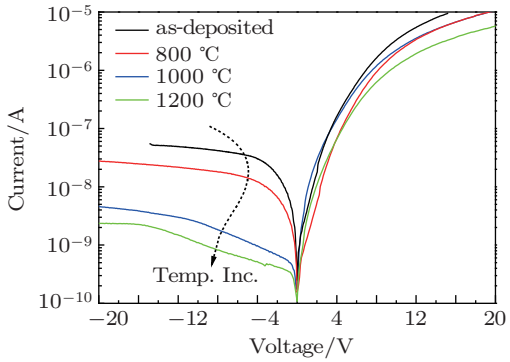


Fig. 5. (color online) *I–V* characteristics for the $Si_{1-x}C_x$/SiC thin films annealed at different annealing temperatures.

4. Conclusion

$Si_{1-x}C_x$/SiC multilayer films were prepared at room temperature by using magnetron sputtering. The as-deposited films were annealed at temperatures ranging from 800 to 1200 °C. The influences of the annealing temperature on the formation of Si and SiC NCs and on the electric characteristics of $Si_{1-x}C_x$/SiC multilayer film were investigated. As-deposited films exhibit an amorphous structure. The subsequent high-temperature annealing induces the changes in the layered structure and electric characteristic and the formation of Si and SiC NCs. XRD and Raman analyses indicate that Si NCs begin to form in samples for $T_a \geq 800$ °C. At annealing temperatures of 1000 °C or greater, the formation of Si NCs was accompanied by the formation of SiC NCs. With the increase of the annealing temperature, the shift of FT-IR

Si–C bond absorption spectra toward a higher wave number along with the change of band shape can be explained by a Si–C transitional phase between the loss of substitutional carbon and the formation of SiC precipitates and a precursor for the growth of SiC crystalline. *C*–*V* and *I*–*V* results indicate that the interface quality between $Si_{1-x}C_x$/SiC multilayer film is improved significantly, and the leakage current is reduced rapidly for $T_a \geq 1000$ °C, which can be assigned to the formation of Si and SiC NCs.

References

[1] Cazzanelli M, Navarro-Urriós D, Riboli F, Daldosso N, Pavesi L, Heitmann J, Yi L X, Scholz R, Zacharias M and Gosele U 2004 *J. Appl. Phys.* **96** 3164

[2] Green M A, Cho E C, Cho Y H, Pink E, Trupke T, Lin K L, Fangsuwannarak T, Puzzer T, Conibeer G and Corkish R 2005 *Proceeding of the* 20*th European Photovoltaic Solar Energy Conference*, June, 2005, Barcelona, Spain, p. 3

[3] Song D, Cho E C, Conibeer G, Cho Y H, Huang Y, Huang S, Flynn C and Green M A 2007 *J. Vac. Sci. Technol. B* **25** 1327

[4] Zhang Q, Zhang Y M, Yuan L, Zhang Y M, Tang X Y and Song Q W 2012 *Chin. Phys. B* **21** 088502

[5] Zhang F S and Li X R 2011 *Chin. Phys. B* **20** 067102

[6] Daldosso N, Das G, Larcheri S, Mariotto G, Dalba G, Pavesi L, Irrera A, Priolo F and Rocca F 2007 *J. Appl. Phys.* **101** 113510

[7] Wang M H, Li D S, Yuan Z Z, Yang D R and Que D L 2007 *Appl. Phys. Lett.* **90** 131903

[8] Kurokawa Y, Miyajima S, Yamada A and Konagai M 2006 *Jpn. J. Appl. Phys.* **45** 1064

[9] Song D, Cho E C, Conibeer G, Huang Y, Flynn C and Green M A 2008 *J. Appl. Phys.* **103** 083544

[10] Wang Y H, Zhang Y M, Zhang Y M, Zhang L, Jia R X and Chen D 2010 *Chin. Phys. B* **19** 036803

[11] Jiang C W and Green M A 2006 *J. Appl. Phys.* **99** 114902

[12] Song D, Cho E C, Conibeer G, Flynn C, Huang Y and Green M A 2008 *Sol. Energy. Mater. Sol. Cells* **92** 474

[13] Song D, Cho E C, Cho Y H, Conibeer G, Huang Y, Huang S and Green M A 2008 *Thin Solid Films* **516** 3824

[14] Zacharias M, Heitmann J, Scholz R, Kahler U, Schmidt M and Bl?sing J 2002 *Appl. Phys. Lett.* **80** 661

[15] Conibeer G, Green M A, Corkish R, Cho Y H, Cho E C, Jiang C W, Fangsuwannarak T, Pink E, Huang Y, Puzzer T, Trupke T, Richards B, Shalav A and Lin K L 2006 *Thin Solid Films* **511** 654

[16] Dhar S, Feldman L C, Wang S, Isaacs-Smith T and Williams J R 2005 *J. Appl. Phys.* **98** 014902

[17] Fernandes M, Vieira M, Rodrignes I and Martins R 2004 *Sensor. Actuat. A* **113** 360

[18] Madani M, Colder H, Portier X, Zellama K, Rizk R and Bouchriha H 2006 *Microelectron. J.* **37** 1031

[19] Tuinstra F and Koenig J L 1970 *J. Chem. Phys.* **53** 1126

[20] Song D Y, Cho E C, Conibeer G, Huang Y D, Flynn C and Green M A 2008 *J. Appl. Phys.* **103** 083544

[21] Lattemann M, Nold E, Ulrich S, Leiste H and Holleck H 2003 *Surf. Coat. Tech.* **174** 365

[22] Wang Y H, Lin J and Huan C H A 2002 *Mater. Sci. Eng. B* **95** 43

[23] Daldosso N, Das G, Larcheri S, Mariotto G, Dalba G, Pavesi L, Irrera A, Priolo F, Lacona F and Rocca F 2007 *J. Appl. Phys.* **101** 113510

[24] Serre C, Calvo-Barrio L, Pérez-Rodríguez A, Romano-Rodríguez A, Morante J R, Pacaud Y, Kögler R, Heera V and Skorupa W 1996 *J. Appl. Phys.* **79** 6907

[25] Kerdiles S, Hairie A, Rizk R and Guedj C 2001 *Phys. Rev. B* **63** 205206

[26] Sha Z D, Wu X M and Zhuge L J 2005 *Vacuum* **79** 250

[27] Dashiell M W, Kulik L V, Hits D A, Kolodzey J and Watson G 1998 *Appl. Phys. Lett.* **72** 833

[28] Mahmood A, Muhl S, Sansores L E and Andrade E 2000 *Thin Solid Films* **373** 180

[29] Serre C, Barrio L C, Rodríguez A P, Rodríguez A R, Morante J R, Pacaud Y, Kogler R, Heera V and Skorupa W 1996 *J. Appl. Phys.* **79** 6907

[30] liveira I C, Massi M, Santos S G, Otani C and Maciel H S 2001 *Diam. Relat. Mater.* **10** 1317